

DMCA: Dense Multi-agent Navigation using Attention and Communication

Senthil Hariharan Arul
Electrical and Computer Engineering
University of Maryland
College Park, United States
sarull@umd.edu

Amrit Singh Bedi
Institute of Systems Research
University of Maryland
College Park, United States
amritbd@umd.edu

Dinesh Manocha
Dept. of Computer Science
University of Maryland
College Park, United States
dmanocha@umd.edu

Abstract—In decentralized multi-robot navigation, the agents lack the world knowledge to make safe and (near-)optimal plans reliably and make their decisions on their neighbors’ observable states. We present a reinforcement learning based multi-agent navigation algorithm that performs inter-agent communications. In order to deal with the variable number of neighbors for each agent, we use a multi-head self-attention mechanism to encode neighbor information and create a fixed-length observation vector. We pose communication selection as a link prediction problem, where the network predicts whether communication is necessary given the observable information. The communicated information augments the observed neighbor information and is used to select a suitable navigation plan. We highlight the benefits of our approach by performing safe and efficient navigation among multiple robots in dense and challenging benchmarks. We also compare the performance with other learning-based methods and highlight improvements in terms of fewer collisions and time-to-goal in dense scenarios.

I. INTRODUCTION

Safe and efficient navigation of multiple robots is at the core of various robotic applications such as warehouse and factory automation, emergency response and rescue, natural resource monitoring, and outdoor industrial operations. These applications benefit from deploying multiple robots in tandem because of improved efficiency and throughput.

A key issue is multi-robot navigation, where the goal is to compute a collision-free trajectory for each robot. This problem has gathered significant attention over the past decade. Its underlying complexity is due to the problem’s large state space associated with the multi-robot system. Centralized and decentralized methods are two primary classes of multi-robot navigation algorithms. Centralized methods [1], [2] view the robots as a single composite system, meaning the central system or server have global knowledge about all the robots. Centralized path generation has gained widespread application in warehouses due to its relative ease of guaranteeing efficient, collision-free paths. However, these methods have limited scalability owing to the central trajectory computation; they are primarily deployable in controlled environments such as warehouses, labs, etc. In the worst case, their computation time can increase exponentially with the number of agents [3], [4]. In decentralized navigation [5]–[7], robots make independent decisions using local sensing or environment. As agents make independent decisions, the computation cost per agent is limited, enabling large-scale deployment. However, decentralized

methods lack global knowledge about other agents and can result in less efficient paths, robot freezing behavior, and even collisions in dense scenarios.

Recently, deep RL-based methods [8], [9] have been developed for multi-agent collision avoidance. In many cases, these RL-based methods can result in improved success rate and time-to-goal, as compared to prior rule-based or model-based methods. RL methods leverage their extensive offline training to learn and map the observation directly into actions. However, they lack explainability and rigorous safety guarantees. Some RL methods [8], [9] use observation vectors containing neighbors’ positions and velocities as network input, similar to model-based methods. In [9], they map the states of the robots and their neighbors to actions by using recurrent neural networks (RNNs) to extract invariant features from the input. However, RNNs tend to focus on recent information rather than treating knowledge of all robots equally.

A. Main Contributions

We present a novel reinforcement learning based multi-agent navigation method. Our approach does not make any assumption about the positions of the agents or their distribution. In order to improve the performance we perform inter-agent communication and use multi-head self-attention mechanism. The novel components of our work include:

- 1) A novel deep reinforcement learning-based method for collision-free navigation in dense multi-robot scenarios.
- 2) To deal with the variable number of neighbors for each robot, we utilize a multi-head attention mechanism to encode the observation vectors from all neighbors to create a fixed-length observation vector.
- 3) We propose a novel scheme to learn with “localized communication” for each robot, which helps improve the overall navigation performance while avoiding collisions.

We evaluate our method on multiple simulated benchmarks to compare its navigation performance against prior learning-based methods [8], [9]. We consider metrics such as path length, time-to-goal, collision rate, and the overall success rate in reaching the goal. We observe up to 24% improvement in success rate over the chosen baseline methods (Section V) in certain scenarios. On average, our method takes ~ 6 ms per

agent to compute the navigation action in scenarios with tens of agents in our benchmarks (Section V-A).

II. RELATED WORK

A. Model-based Collision Avoidance

Fiorini and Shiller presented the velocity obstacle (VO) [10] concept, which computes collision-free velocities for the agents based on their observations of neighbors' positions and velocities. RVO [6] improves on VO by incorporating reciprocity in terms of velocity computation. Further, ORCA [5] linearizes the RVO constraints to improve computational efficiency. Many extensions of velocity obstacles have been proposed that impose dynamics constraints [11]. BVC [7] constructs a Voronoi-based free space for each agent to perform collision-free navigation. V-RVO [12] presents a hybrid between RVO and BVC for improved collision avoidance performance.

B. Learning-based Collision Avoidance

The idea of utilizing deep RL to achieve better navigation performance has been investigated in the literature. CADRL [8] proposed an RL method for multi-agent navigation, which showed improved time-to-goal performance compared to ORCA. Semnani et al. [13] presented a hybrid-framework that switches between RL and force-based planning based on the scene complexity, resulting in an improved success rate and time-to-goal. Everett et al. [9] further improved CADRL to account for an arbitrary number of neighboring agents by using an LSTM to encode a varying-size observation vector into a fixed length vector. In [14], a self-attention mechanism is used to aggregate pairwise interactions. In contrast, our method uses multi-head self-attention [15] to encode the observation to a fixed length vector. Self-attention is independent of sequence order, unlike LSTM.

Long et al. [16] learn to map raw sensor data to action. The method shows a better success rate, path optimality, agent's average speed, and time-to-goal than NH-ORCA [17]. Fan et al. [18] further improved the performance by adopting a hybrid framework. DRL-VO [19] uses a velocity obstacle (VO) based cost in the rewards to improve the success rate. Han et al. [20] presented a DRL method with an RVO-shaped reward for better reciprocal behavior.

Li et al. [21] proposed a hybrid method based on RL and ORCA. The RL network computes the desired action for each neighboring agent, weighted to compute a suitable preferred velocity used in the ORCA formulation. Riviere et al. [22] presented a distributed, provably safe policy generation for multi-agent planning that uses globally planned trajectories, constructs a local observation action training set, and is used to learn a decentralized policy using deep imitation learning. A safety module based on control barrier function (CBF) trains the network end-to-end to ensure collision-free navigation. Cai et al. [23] propose CBF-based shielding for safety-critical MARL tasks. DeepMNavigate [24] proposes to use both global and local information about the environments to navigate and shows improved performance in dense scenarios.

In contrast to existing deep RL based approaches, our proposed network uses a multi-head self-attention module to encode the neighbor information. Besides, our agents are allowed to communicate with neighbors to improve their decision-making. Our network includes a communication module that communicates with select neighbors at any time. This improves the overall navigation performance.

III. PROBLEM FORMULATION AND OVERVIEW

This section lists our assumptions, summarizes our problem statement, and provides an overview of our approach. Table I lists the common symbols and notations used in our paper.

A. Assumptions

In this paper, we assume disk-shaped robots with unicycle dynamics. We consider a request-reply type communication between the ego-agent and its neighbors. That is, an agent request its neighbor for information, and the neighbor replies with the information. Also, we use ego-agent to refer to the agent being considered. We assume the request-reply is fast and executed within a single planning cycle.

Symbols	Description
\mathbf{p}_i	Position of agent i (p_x, p_y)
\mathbf{v}_i	Velocity of agent i (v_x, v_y)
ψ_i	Heading of agent i
r_i	Radius of agent i
v_{pref_i}	Preferred Velocity of agent i
\mathbf{g}_i	Goal of agent i (g_x, g_y)
\mathcal{N}_i	Set of neighbors of agent i
\mathcal{C}_i	Set of selected neighbors for communication

TABLE I: Symbols

B. Problem Statement

We consider the problem of cooperative multi-robot navigation where robots can communicating with each other. We propose a deep RL method to navigate individual robots towards their respective goals while avoiding collisions. Each robot communicates with its neighbors to obtain information to improve their navigation decisions. Mathematically, let us consider an environment $\mathcal{W} \subset \mathbb{R}^2$ with N communicating robots $\{\mathcal{A}_1, \mathcal{A}_2, \dots, \mathcal{A}_n\}$. Each robot is a disk-shaped robot with 2D position $\mathbf{p}_i \in \mathcal{W}$, radius r_i , and goal $\mathbf{g}_i \in \mathcal{W}$. Let t denotes the time step, then we can express the per step safe-navigation problem for robot i as follows:

$$\arg \min_{\pi_i} \|\mathbf{p}_i(t) - \mathbf{g}_i\| \quad (1)$$

$$\|\mathbf{p}_i(t) - \mathbf{p}_j(t)\|_2 \geq r_i + r_j \quad (2)$$

$$\forall i, j \in \{1, 2, \dots, N\}, i \neq j \quad \forall t. \quad (3)$$

Here, $\mathbf{p}_i(t)$ represents the path of the robot i as a function of time t , and π_i is the policy navigating the robot. Following the definition from CADRL [8], the agent's state $\mathbf{s}_i = [\mathbf{s}_i^o, \mathbf{s}_i^h]$ includes an observable component and a hidden component. The observable component \mathbf{s}_i^o includes the agent's position, velocity, and radius. The hidden component \mathbf{s}_i^h includes the

agent's goal, preferred speed, and current orientation. Hence, we represent them as:

$$\mathbf{s}_i^o = [p_x, p_y, v_x, v_y, r], \quad \mathbf{s}_i^h = [g_x, g_y, v_{pref}, \psi].$$

The agent's control input includes its speed and heading angle and is given by $\mathbf{u}_i = [v_i, \psi_i]$.

C. Multi-head Attention

Initially proposed in [15], self-attention has shown immense potential in natural language processing and computer vision. Self-attention mechanism compares elements of an input sequence with each other to compute a representation of the sequence. For each element in the input sequence, the attention mechanism calculates Query (Q), Key (K), and Value (V) vectors by multiplying them with trained matrices. Using the Q, K, and V vectors, a self-attention score is computed for each element in the sequence. The score determines the focus awarded to other sequence elements for encoding a particular element, we can write

$$Attention(Q, K, V) = \left(\frac{QK^T}{\sqrt{d_k}} \right) V,$$

where, $\sqrt{d_k}$ is the dimension of K.

In multi-head attention [15], multiple heads are created by linearly projecting Q, K, and V. Each self-attention head focuses on different subspaces, and attention is performed in parallel. The projected queries, keys, and values are fed into attention pooling in parallel. Next, attention pooling outputs are concatenated and transformed with another learned linear projection to produce the final output. Hence, we can write

$$\text{Multi-head}(Q, K, V) = \text{Concat}(\text{head}_1, \text{head}_2, \dots, \text{head}_k) W^O,$$

$$\text{head}_i = \text{Attention}(QW_i^Q, KW_i^K, VW_i^V),$$

where W_i^Q, W_i^K, W_i^V, W^O are parameter matrices for projection. Prior works, like [9], use LSTM to encode the observation, but LSTMs are known to focus more on the recent input. Using self-attention can avoid the encoding being order dependent.

D. Inter-agent Communications

Communication in a multi-agent setting involves transferring information such as state, intent, or observations between the agents. Communication is primarily either broadcast or selective. In broadcast, an agent publishes its information to be used by all agents. In selective, the agents make intelligent decisions about when and with whom to communicate. A few works have explored communication in the multi-agent navigation domain. Serra-Gómez [25] learns whom to communicate with and requests the planned trajectories from the chosen neighbor to be used in the MPC planner. Ma et al. [26] present a DRL method for multi-agent pathfinding with broadcast communication. [27] reduces the communication overhead by combining the idea of I2C [28] for multi-agent navigation in a grid world domain.

In our formulation, the agents communicate their hidden state (Section III-E), which includes the goal location of the agent. Communicating goal location provides the intent of the agent to its neighbors.

E. Reinforcement Learning

As with prior methods [8], [9], we consider a local coordinate frame with the state composed of information about the ego-agent and its neighbors. The information about the ego-agent includes its distance to the goal, preferred speed, orientation, and radius as

$$\mathbf{s}^{ego} = [||\mathbf{g}_i - \mathbf{p}_i||, v_{pref_i}, \psi_i, r_i].$$

The world information includes the agent's neighbors, including their positions, velocities w.r.t the ego frame, radii, inter-agent distances, and combined radii denotes as

$$\begin{aligned} \mathbf{s}^{obs_j} &= [p_{x_j}, p_{y_j}, v_{x_j}, v_{y_j}, r_j, d_a, r_i + r_j], \\ \mathbf{s}^{obs} &= [\mathbf{s}^{obs_1}, \mathbf{s}^{obs_2}, \dots, \mathbf{s}^{obs_n}] \quad 1, 2, \dots, n \in \mathcal{N}_i. \end{aligned}$$

In addition, our method allows the agent to request one or more of its neighbors for their hidden state (\mathbf{s}_j^h) using communication to augment the network's input. The communicated information is used to construct a communicated state from each neighbor and includes dist to a neighbor's goal from the ego-agent, the difference in preferred speeds between the ego-agent and its neighbor, and relative orientation/heading. More details are presented in Section IV-B

Based on the prior approach [9], our multi-agent RL problem formulation is trained with GA3C and uses a similar navigation reward. We positively reward the agents for reaching the goal and negatively reward them for a collision and close proximity to other agents. d_{min} is the closest neighbor distance. In addition, for DMCA-LC model (described in Section V) we have a negative reward for every communication link.

$$R = \begin{cases} 1.0, & p_i = g_i \\ -0.25, & \text{collision} \\ -0.1 + d_{min}/2 & \text{if } d_{min} < 0.2 \\ -0.0001 \cdot n_l & n_l: \text{no of comm. links} \\ 0.0, & \text{otherwise} \end{cases} \quad (4)$$

IV. DMCA: MULTI-AGENT RL NAVIGATION

In this section, we illustrate our proposed network architecture (Figure 1) and describes its modules. Our network consists of 3 components: the observation encoder, the communication module, and the navigation module. The observation encoder performs the task of encoding neighbors' information for use in the policy. The communication module links with neighbors to obtain their hidden states, resulting in more information about the world for the ego-agent. The navigation module maps the encoded vectors to a distribution over the action space.

A. Observation Encoding

The observation encoder takes the observation vector of all neighboring robots (\mathbf{s}^{obs_j}) as input to create a fixed-length vector for input to the navigation module. Since the number of neighbors around an agent varies at any point in time, our method needs to account for varying numbers of agents. Thus, our observation encoder uses a multi-head self-attention

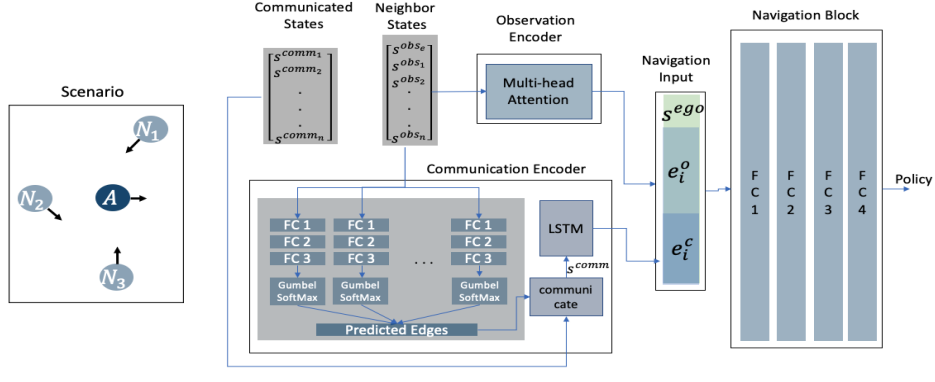


Fig. 1: We illustrate the high-level network architecture used for multi-agent navigation in DCMA. Primarily, the network consists of three modules: the observation encoder, the communication selection, and the navigation block.

to encode the neighbors s^{obs_j} into a fixed-length observation vector.

The input sequence consists of s^{obs_j} for each neighbor, which is represented relative to the ego agent. In addition, we compute $s^{obs_{ego}}$, which is the observed state of the ego agent relative to the ego frame. The ego-agent's observed state is needed for our self-attention mechanism. Based on the ego observed state, we identify the attention paid to neighboring observed states, which is combined to produce the encoded vector. The input sequence consists of the ego agent's observable state, followed by its neighbors' observable state. Finally, the representation computed for $s^{obs_{ego}}$ is used as the encoded representation.

$$e^o = \text{encode}([s^{obs_{ego}}, s^{obs}])$$

Our encoder uses 20 heads for our observation encoding module, with Key, Query encoding using a dense layer with 128 nodes; the Value has 256 nodes.

B. Communication Selection

This block performs communication selection using the robot's local observation. We formulate the communication selection as a link prediction problem between the ego robot and its neighbors. The set of neighbors for an agent i is given by $\mathcal{N}^i = \{j \mid j \neq i, \|\mathbf{p}_j - \mathbf{p}_i\| < r_{neighbor}\}$, where $r_{neighbor}$ represents a radius threshold. The module takes the neighbor's observable states as input and individually passes them through a series of three fully connected layers. Since s^{obs_j} is in relative frame w.r.t to the ego agent, we pass the vector through a sequential layer to predict the possibility of a communication link.

In this regard, the output of the sequential layer has 2 nodes, one indicating the probability of a link (p_{link}) and the other node indicating $1 - p_{link}$. The first 2 layers have 64 nodes and relu activation, with the last layer having 2 output nodes and softmax activation. The Gumbel-Softmax [29], [30] layer is used to sample a discrete distribution based on the probability of a link.

$$\forall j \in \mathcal{N}^i \quad [p_{link_j}, 1 - p_{link_j}] = \text{Comm. Sel}(s^{obs_j}). \quad (5)$$

Thus, for each neighbor, the communication module predicts a communication link. If a link is predicted, the agent sends a communication request to the selected neighbors. The neighbors respond with the hidden states of the agents $s^h = [g_x, g_y, v_{pref}, \psi]$.

The received hidden states are combined with the observed states from the neighbors to create a communication state. The communication state is given by,

$$s^{comm_j} = [\|\mathbf{g}_j - \mathbf{p}_i\|, v_{pref_j} - v_{pref_i}, \psi_j - \psi_i] \quad j \in \mathcal{N}^i$$

$$s^{comm} = \begin{bmatrix} [s^{obs_1}, s^{comm_1}], [s^{obs_2}, s^{comm_2}], \dots, \\ [s^{obs_n}, s^{comm_n}] \end{bmatrix} \quad 1, 2, \dots, n \in \mathcal{C}_i.$$

We pass the communication vector through an LSTM to create an encoded vector e^c .

$$e^c = \text{LSTM}(s^{comm_j})$$

C. Navigation Input

The navigation input consists of three important vectors: the host agent state, the encoded observation vector, and the encoded communication vector, and is the input to the navigation module.

$$s^{input} = [s^{ego}, e^o, e^c]$$

D. Navigation

Our navigation module consists of a sequential layer with 4 fully connected layers. The first layer has 1024 nodes, the next two layers have 512 node, and the last layer has 256 nodes. As in [9], the output from the final layers includes the scalar value function and the distribution over the action space.

V. EVALUATION

A. Computational Setup

Our method was implemented on an Intel Xeon 4208 CPU with 32 GB RAM and a Nvidia GeForce RTX 2080 Ti graphic card. We use TensorFlow and Python for the deep learning

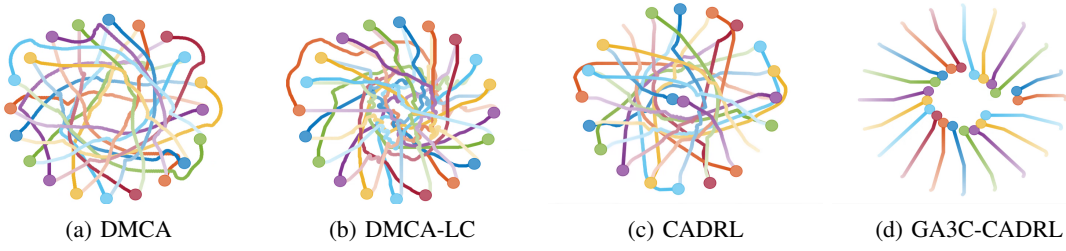


Fig. 2: We compare the trajectories generated by our proposed method (DCMA) with CADRL and GA3C-CADRL for a circular scenario with 20 agents. We observe that DCMA generates smooth and collision-free trajectories to the goal, while CADRL results in some collisions. In GA3C-CADRL, some agents were deadlocked while others were in a collision, and no agent reached the goal. The network requires 6 ms per agent to compute an action.



Fig. 3: We consider a complex scenario where the robots are arranged in $n \times n$ grid formation. The final formation is created by moving the robot at position (row, column) to $(n - \text{row} + 1, n - \text{column} + 1)$. The figure from left to right shows the progression of the agents moving from the initial to final configuration. We observe DMCA can generate collision-free trajectories to the final configuration. Prior learning methods may not work well on these benchmarks.



Fig. 4: We consider a swap scenario with disk shaped static obstacles (black) and eight agents. We observe the eight agents using DMCA remain safe and successfully reach their goal in this scenario.

implementation. We use gym-collision avoidance and GA3C-CADRL package [31] to implement our method and for our evaluations.

We train in a curriculum setup. Initially the robot is trained in a scenario with 4 agents. The training scenario is random, with examples of circle scenarios, random start and stop, etc. In phase 2 the agent number is increased to 8. The Training process took 2 days to converge on our setup.

B. Baselines

We compare our method against prior model- and learning-based decentralized methods. We choose RVO [6], CADRL [8], and GA3C-CADRL [9] as our baselines for comparison. We present two version of our algorithm: 1) DMCA: trained without the negative reward for communication link and 2) DMCA-LC, which has limited communication: A model trained with the negative reward for communication link. We observe the first model (DMCA) results in a communication frequently, while the the other model (DMCA-LC) is more conservative in terms of communicating with neighbors.

C. Trajectories

In figure 2, we compare the generated trajectories between our proposed methods DMCA and DMCA-LC with CADRL



Fig. 5: The figure illustrates the trajectories for robots traveling through a narrow passage. The narrow passage is create by two circular disk (red and black). We observe DMCA successfully navigates the robots to the final configuration in such narrow spaces.

and GA3C-CADRL. In this scenario, we observe DMCA to result in smoother trajectory than DMCA-LC. Besides, the other learning methods result in collisions. In figures 3, 4, and 5 we shows the trajectories generated by DMCA in three benchmarks one involving a grid formation, one with static obstacle, and the other involving narrow passage. DMCA navigated the agents safely in these cases.

D. Collision Rate, Success Rate and Time-to-goal

We compare the proposed method with other baselines in terms of the number of collisions, time to goal, and success rate in reaching the goal formation. We define the success rate

Robots	Collision Rate					Time to Goal					Success Rate				
	4	6	10	20	30	4	6	10	20	30	4	6	10	20	30
Scenario 1: Circle Scenario (agent radius 0.2m)															
DMCA	0.00	0.00	0.00	0.00	0.05	113.2	114.6	114.2	201.6	242.3	1.00	1.00	1.00	1.00	0.95
DMCA-LC	0.00	0.00	0.00	0.43	0.45	144.3	125.2	124.2	NR	NR	1.00	1.00	1.00	0.57	0.55
RVO [6]	0.00	0.00	0.00	0.02	0.50	109.2	116.2	118.4	214.8	NR	1.00	1.00	1.00	0.98	0.36
CADRL [8]	0.00	0.00	0.00	0.00	0.00	108.0	111.5	126.3	201.2	212.8	1.00	1.00	1.00	1.00	0.99
GA3C [9]	0.10	0.30	0.62	0.90	0.97	108.3	109.8	NR	NR	NR	0.90	0.70	0.37	0.10	0.03
Scenario 1: Circle Scenario (agent radius 0.5m)															
DMCA	0.00	0.00	0.00	0.00	0.00	114.7	117.5	144.3	242.0	276.0	1.00	1.00	1.00	1.00	0.99
DMCA-LC	0.00	0.00	0.00	0.10	0.32	123.8	127.4	166.6	287.0	NR	1.00	1.00	1.00	0.90	0.63
RVO [6]	0.00	0.00	0.00	0.00	0.02	116.1	134.2	199.1	327.5	NR	1.00	1.00	1.00	1.00	0.75
CADRL [8]	0.00	0.00	0.31	0.15	0.31	105.6	108.1	136.7	194.0	NR	1.00	1.00	0.67	0.85	0.57
GA3C [9]	0.35	1.00	1.00	1.00	1.00	104.0	NR	NR	NR	NR	0.65	0.00	0.00	0.00	0.00

TABLE II: We tabulate the collision rate, time to goal, and success rate for circle scenarios. The maximum simulation time is 500 time steps, the success rate is computed based on the number of agents reaching the goal before the simulation ends. The results are averaged over 20 trials. The average time to goal is computed based on the trials where all robots reach their goal. If no successful trials were observed, we report ‘NR’ as time-to-goal as robot have not reached final configuration. We observe DCMA to provide better success rate in the circle scenario with agent radius of 0.5m.

Scenario 2: Swap Scenario															
Robots	Collision Rate					Time to Goal					Success Rate				
	4	6	10	20	30	4	6	10	20	30	4	6	10	20	30
DMCA	0.00	0.00	0.00	0.00	0.00	123	136	153	NR	NR	1.00	1.00	1.00	0.70	0.73
DMCA-LC	0.00	0.00	0.00	0.00	0.17	122	136	146	NR	NR	1.00	1.00	1.00	0.75	0.60
RVO [6]	0.00	0.00	0.00	0.00	0.00	116	161	160	NR	NR	1.00	1.00	1.00	0.60	0.63
CADRL [8]	0.00	0.00	0.00	0.00	0.27	106	113	129	NR	NR	1.00	1.00	1.00	0.65	0.57

TABLE III: The collision rate, time-to-goal, and success rate for the swap scenario. The maximum simulation time is 500 steps. In practice, DCMA exhibits the best overall performance.

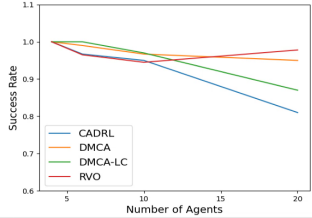


Fig. 6: Success Rate: Plot illustrates the variation of success rate with number of agents for our proposed method, CADRL [8] and RVO [6]. We observe that our approach (DMCA) results in good success rate.

as the number of agents that reach the goal without collision or deadlock. We consider two scenarios: 1) A circle scenario with agents placed on the perimeter of a circle and 2) A swap scenario where the agents are initially arranged into two columns. The agents on the left and right columns are made to swap with each other. Tables II and III summarize our observations.

Scenario 1 (Circle): In the circle scenario, we observe our proposed method results in the fewest collisions compared to the other learning methods. With regards to the time-to-goal, CADRL results in a shorter time-to-goal in the scenarios where the agents remained collision-free.

Scenario 2 (Swap): We observed lower collisions and higher success rate in our method compares to other baselines. The time to goal values are higher compared to CADRL.

E. Random Scenario

In this evaluation, we consider a scenario with random start and end points with agents of random radii. In figure 6, we plot the success rate (averaged over 50 trials) with respect to

Agents	DMCA	DMCA-LC
2	76	1
4	234	13
6	252	59
8	311	149

TABLE IV: Number of communication links made by a single agent in circle scenario. DMCA-LC significantly reduced the number of pairwise communications.

the number of agents. We observe DMCA results in a higher success rate in comparison to other learning based methods.

F. Communication links

We compare DMCA and DMCA-LC to compare the effect of using a negative reward for communication. In table IV, we tabulate the number of communication a single agent makes in circle scenario. In this scenario, an agent can communicate with 3 agents at a maximum at any time step. We observe in DMCA-LC uses significantly less communication compared to DMCA.

VI. CONCLUSION, LIMITATION, AND FUTURE WORK

We proposed a collision avoidance method for multi-agent navigation with communication. Our method uses communication to transfer hidden state information between agents to improve their navigation performance. We use a self-attention model to encode neighbor observation, and perform link prediction to perform inter-agent communication. Our method shown to outperform other learning-based baseline in simulation on multiple scenarios. As future work, we plan to test the method on a fleet of physical robots. This work attempts to answer the use of communication in navigation, and we plan to develop better models of learning communication. We would also like to extend to scenarios with noisy sensors.

REFERENCES

- [1] S. Tang and V. Kumar, "A complete algorithm for generating safe trajectories for multi-robot teams," in *Robotics Research*. Springer, 2018, pp. 599–616.
- [2] W. Hönig, J. A. Preiss, T. K. S. Kumar, G. S. Sukhatme, and N. Ananyan, "Trajectory planning for quadrotor swarms," *IEEE Transactions on Robotics*, vol. 34, no. 4, pp. 856–869, 2018.
- [3] K. Solovey, O. Salzmann, and D. Halperin, "Finding a needle in an exponential haystack: Discrete rrt for exploration of implicit roadmaps in multi-robot motion planning," *The International Journal of Robotics Research*, vol. 35, no. 5, pp. 501–513, 2016.
- [4] M. Goldenberg, A. Felner, R. Stern, G. Sharon, N. Sturtevant, R. C. Holte, and J. Schaeffer, "Enhanced partial expansion a," *Journal of Artificial Intelligence Research*, vol. 50, pp. 141–187, 2014.
- [5] J. v. d. Berg, S. J. Guy, M. Lin, and D. Manocha, "Reciprocal n-body collision avoidance," in *Robotics research*. Springer, 2011, pp. 3–19.
- [6] J. Van den Berg, M. Lin, and D. Manocha, "Reciprocal velocity obstacles for real-time multi-agent navigation," in *2008 IEEE international conference on robotics and automation*. Ieee, 2008, pp. 1928–1935.
- [7] D. Zhou, Z. Wang, S. Bandyopadhyay, and M. Schwager, "Fast, on-line collision avoidance for dynamic vehicles using buffered voronoi cells," *IEEE Robotics and Automation Letters*, vol. 2, no. 2, pp. 1047–1054, 2017.
- [8] Y. F. Chen, M. Liu, M. Everett, and J. P. How, "Decentralized non-communicating multiagent collision avoidance with deep reinforcement learning," in *2017 IEEE International Conference on Robotics and Automation (ICRA)*, 2017, pp. 285–292.
- [9] M. Everett, Y. F. Chen, and J. P. How, "Collision avoidance in pedestrian-rich environments with deep reinforcement learning," *IEEE Access*, vol. 9, p. 10357–10377, 2021. [Online]. Available: <http://dx.doi.org/10.1109/ACCESS.2021.3050338>
- [10] P. Fiorini and Z. Shiller, "Motion planning in dynamic environments using velocity obstacles," *The international journal of robotics research*, vol. 17, no. 7, pp. 760–772, 1998.
- [11] D. Bareiss and J. Van den Berg, "Generalized reciprocal collision avoidance," *The International Journal of Robotics Research*, vol. 34, no. 12, pp. 1501–1514, 2015.
- [12] S. H. Arul and D. Manocha, "V-rvo: Decentralized multi-agent collision avoidance using voronoi diagrams and reciprocal velocity obstacles," in *2021 IEEE/RSJ International Conference on Intelligent Robots and Systems (IROS)*, 2021, pp. 8097–8104.
- [13] S. H. Semnani, H. Liu, M. Everett, A. de Ruiter, and J. P. How, "Multi-agent motion planning for dense and dynamic environments via deep reinforcement learning," *IEEE Robotics and Automation Letters*, vol. 5, no. 2, pp. 3221–3226, 2020.
- [14] C. Chen, Y. Liu, S. Kreiss, and A. Alahi, "Crowd-robot interaction: Crowd-aware robot navigation with attention-based deep reinforcement learning," in *2019 International Conference on Robotics and Automation (ICRA)*. IEEE, 2019, pp. 6015–6022.
- [15] A. Vaswani, N. Shazeer, N. Parmar, J. Uszkoreit, L. Jones, A. N. Gomez, Ł. Kaiser, and I. Polosukhin, "Attention is all you need," *Advances in neural information processing systems*, vol. 30, 2017.
- [16] P. Long, T. Fan, X. Liao, W. Liu, H. Zhang, and J. Pan, "Towards optimally decentralized multi-robot collision avoidance via deep reinforcement learning," in *2018 IEEE International Conference on Robotics and Automation (ICRA)*, 2018, pp. 6252–6259.
- [17] J. Alonso-Mora, A. Breitenmoser, M. Ruffli, P. Beardsley, and R. Siegwart, "Optimal reciprocal collision avoidance for multiple non-holonomic robots," in *Distributed autonomous robotic systems*. Springer, 2013, pp. 203–216.
- [18] T. Fan, P. Long, W. Liu, and J. Pan, "Distributed multi-robot collision avoidance via deep reinforcement learning for navigation in complex scenarios," *The International Journal of Robotics Research*, vol. 39, no. 7, pp. 856–892, 2020. [Online]. Available: <https://doi.org/10.1177/0278364920916531>
- [19] Z. Xie and P. Dames, "Drl-vo: Using velocity obstacles to learn safe navigation policies for crowded dynamic scenes."
- [20] R. Han, S. Chen, S. Wang, Z. Zhang, R. Gao, Q. Hao, and J. Pan, "Reinforcement learned distributed multi-robot navigation with reciprocal velocity obstacle shaped rewards," *IEEE Robotics and Automation Letters*, vol. 7, no. 3, pp. 5896–5903, 2022.
- [21] H. Li, B. Weng, A. Gupta, J. Pan, and W. Zhang, "Reciprocal collision avoidance for general nonlinear agents using reinforcement learning," 2020.
- [22] B. Rivière, W. Hönig, Y. Yue, and S.-J. Chung, "Glas: Global-to-local safe autonomy synthesis for multi-robot motion planning with end-to-end learning," *IEEE Robotics and Automation Letters*, vol. 5, no. 3, pp. 4249–4256, 2020.
- [23] Z. Cai, H. Cao, W. Lu, L. Zhang, and H. Xiong, "Safe multi-agent reinforcement learning through decentralized multiple control barrier functions," 2021.
- [24] Q. Tan, T. Fan, J. Pan, and D. Manocha, "Deepmnavigate: Deep reinforced multi-robot navigation unifying local & global collision avoidance," in *2020 IEEE/RSJ International Conference on Intelligent Robots and Systems (IROS)*, 2020, pp. 6952–6959.
- [25] A. Serra-Gomez, B. Brito, H. Zhu, J. J. Chung, and J. Alonso-Mora, "With whom to communicate: Learning efficient communication for multi-robot collision avoidance," in *2020 IEEE/RSJ International Conference on Intelligent Robots and Systems (IROS)*, 2020, pp. 11 770–11 776.
- [26] Z. Ma, Y. Luo, and H. Ma, "Distributed heuristic multi-agent path finding with communication," in *2021 IEEE International Conference on Robotics and Automation (ICRA)*, 2021, pp. 8699–8705.
- [27] Z. Ma, Y. Luo, and J. Pan, "Learning selective communication for multi-agent path finding," *IEEE Robotics and Automation Letters*, vol. 7, no. 2, pp. 1455–1462, 2021.
- [28] Z. Ding, T. Huang, and Z. Lu, "Learning individually inferred communication for multi-agent cooperation," in *Advances in Neural Information Processing Systems*, H. Larochelle, M. Ranzato, R. Hadsell, M. Balcan, and H. Lin, Eds., vol. 33. Curran Associates, Inc., 2020, pp. 22 069–22 079.
- [29] E. Jang, S. Gu, and B. Poole, "Categorical reparameterization with gumbel-softmax," 2016. [Online]. Available: <https://arxiv.org/abs/1611.01144>
- [30] C. J. Maddison, A. Mnih, and Y. W. Teh, "The concrete distribution: A continuous relaxation of discrete random variables," 2016. [Online]. Available: <https://arxiv.org/abs/1611.00712>
- [31] M. Everett, Y. F. Chen, and J. P. How, "Motion planning among dynamic, decision-making agents with deep reinforcement learning," in *IEEE/RSJ International Conference on Intelligent Robots and Systems (IROS)*, Madrid, Spain, Sep. 2018. [Online]. Available: <https://arxiv.org/pdf/1805.01956.pdf>